



HAL
open science

Absorption spectra of alkali-C-60 nanoclusters

Franck Rabilloud

► **To cite this version:**

Franck Rabilloud. Absorption spectra of alkali-C-60 nanoclusters. *Physical Chemistry Chemical Physics*, 2014, 16, pp.22399-22408. 10.1039/c4cp03352c . hal-02309839

HAL Id: hal-02309839

<https://univ-lyon1.hal.science/hal-02309839>

Submitted on 18 Jan 2020

HAL is a multi-disciplinary open access archive for the deposit and dissemination of scientific research documents, whether they are published or not. The documents may come from teaching and research institutions in France or abroad, or from public or private research centers.

L'archive ouverte pluridisciplinaire **HAL**, est destinée au dépôt et à la diffusion de documents scientifiques de niveau recherche, publiés ou non, émanant des établissements d'enseignement et de recherche français ou étrangers, des laboratoires publics ou privés.

Absorption spectra of alkali-C₆₀ nanoclusters

Franck Rabilloud

Institut Lumière Matière, UMR5306 Université Lyon 1 – CNRS,

Université de Lyon, 69622 Villeurbanne Cedex, France;

franck.rabilloud@univ-lyon1.fr

tel. 33 4 72 43 29 31

fax. 33 4 72 43 15 07

Date: September 3th, 2014

Abstract:

We investigate the absorption spectra of alkali-doped C₆₀ nanoclusters, namely C₆₀Na_n, C₆₀K_n, and C₆₀Li_n, with n=1, 2, 6, 12, in the framework of the Time-Dependent Density-Functional Theory (TDDFT). We study the dependence of the absorption spectra on the nature of the alkali. We show that in few cases the absorption spectra depend on the arrangement of the alkali atoms over the fullerene, though sometimes the absorption spectra do not allow to distinguish between different configurations. When only one or two alkali atoms are adsorbed on the fullerene, the optical response of alkali-doped C₆₀ is similar to that of the anion C₆₀⁻ with a strong response in the UV domain. In contrast, for higher concentration of alkali, a strong optical response is predicted in the visible range, particularly when metal-metal bonds are formed. The weak optical response of the *I_h*-symmetry C₆₀Li₁₂ is proposed to be used as a signature of its structure.

Keywords:

alkali-C₆₀, C₆₀, fullerenes, alkali, Absorption spectra, TDDFT

1. Introduction

The discovery of C_{60} by Smalley and co-workers [1] gave birth to new fields of research ranging from molecular chemistry to materials and condensed matter physics. In particular, the interaction between fullerenes and alkali atoms has attracted a lot of attention since the discovery of superconductivity in the potassium- C_{60} [2] and rubidium- C_{60} [3] fullerides. More recently, the doping of alkali metal atoms on fullerenes was shown to cause a remarkable enhancement in the hydrogen adsorption capacity and was suggested as a possible route toward hydrogen storage materials [4-11]. The charge transfer from the alkali atom to the fullerene cage leaves the alkali atom in a cationic state which can then bind H_2 molecules due to polarization forces. However, when several alkali atoms lie a fullerene, the hydrogen adsorption capacity greatly depends on the wetting or nonwetting of the fullerene surface with alkali atoms: an homogenous coating of the fullerene by the alkali atoms is expected to be much more efficient than the growth of a metallic droplet not wetting the fullerene surface which could drastically limit the amount of stored hydrogen.

Many experimental and theoretical studies have been devoted to the electronic and structural properties of $C_{60}M_n$ clusters, with $M=Li, Na, K$ [12-28]. Very early, the strong stability of $C_{60}Li_{12}$ was interpreted as a signature of a homogeneous coating of the fullerene by all lithium atoms above the twelve pentagonal faces of the C_{60} molecule resulting in an icosahedral arrangement [12-14]. In contrast, coating the fullerene with sodium or potassium atoms led to an even - odd alternation in the mass spectra, suggesting the onset of metallic bonding. Following previous theoretical studies [13,17,19-22] achieved with some limitations or constraints (for examples, use of a many-body force field without explicit electronic structure or first principles calculations assuming a rigid C_{60} cage), we have recently performed geometry optimizations in the framework of the density-functional theory (DFT), without any constraint, of selected initial configurations ranging from homogeneous covering of the fullerene to complete segregation in which alkali atoms form a droplet not wetting the fullerene surface, and also intermediate situations [24-25]. The structures of Li_n -, Na_n - and K_n - coated C_{60} fullerene with $n=1, 2, 6, 12$ were investigated. The optimization process involved the fullerene structure. Our calculations have confirmed that lithium atoms coat homogeneously the fullerene on the C_{60} surface via pentagonal sites (at least up to 12 alkali atoms), contrary to sodium and potassium atoms which prefer to form 4-atom islands on the surface [24, 25]. However, in some

cases, several configurations were found to compete for the lowest-energy isomers and to be degenerate. The degeneracy of the most stable structures were found to result from a balance between the electrostatic repulsion, due to the electronic charge transfer from the metal atoms to C_{60} versus the residual metallic bonding.

The goal of the present study is to characterize the absorption spectra of the most stable configurations of C_{60} -alkali complexes. We will show that in few cases the absorption spectra depend on the nature of alkali and also on the arrangement of the alkali atoms over the fullerene, though sometimes the absorption spectra do not allow to distinguish between different configurations. Complexes investigated here include $C_{60}M_n$ with $M = \text{Li, Na, K}$, and $n = 1, 2, 6, 12$. In the following section, we give some details of calculations, and then we will present our results.

2. Computational details

The cluster geometries were taken from our previous works [24, 25]. They were optimized by use of the hybrid B3LYP functional [29, 30] with Gaussian basis sets of double zeta valence quality. In the optimization process of cluster geometries, a number of structures were tested for each size. Only selected initial geometries in which alkali atoms in contact with C_{60} are above either the center of a pentagonal ring or a hexagonal ring were considered, since the top- or bridge-site type were previously shown to be unfavorable. Of course all the possible configurations had not been explored due to the prohibitive cost of calculations. However, the studied configurations were selected in order to provide different situations ranging from the homogeneous covering of the fullerene to complete segregation and also intermediate situations. All optimizations were carried out without symmetry constraints (C_1 point group). In the present work, we have only considered the most representative configurations among the lowest-energy isomers for each complex. The relative energies of each isomer are given in Table 1, and the structures are showed in the figures below.

Absorption spectra were calculated with the GAUSSIAN09 program package [31] in the framework of the time-dependent density-functional theory [32-34] (TDDFT). To give an accurate description of the charge-transfer excited states [35], we have used a long-range corrected hybrid functional namely CAM-B3LYP [36]. Calculations were achieved in the linear combination of atomic orbitals scheme. All atoms were described with the 6-31G(d) basis sets

[37-39]. The absorption spectra showed in the next section give the oscillator strength as a function of the excitation energy together with a curve obtained by a Lorentzian broadening with a full width at half maximum (fwhm) of 0.05 eV. For each species, we present spectra including calculated excitation energies up to the vertical ionization potential (IP) of the lowest-energy isomer. IPs, given in Table 1, are calculated at CAM-B3LYP/6-31G(d) level. The performance of the present level of calculation was evaluated with several tests (see Supplementary information). Spectra of $C_{60}Li_2$ and $C_{60}Na_2$ calculated with a basis set enriched by more diffuse functions, namely 6-31+G(d), are found to be very similar to those obtained with the 6-31G(d) basis set. Several exchange and correlation functionals have been tested including the hybrid B3LYP and PBE0 [40], and the long-range-corrected ones ω B97x [41], LC-M06L($\omega=0.33$) [42,43,35], LC- ω PBE($\omega=0.40$) [44]. Spectra of $C_{60}Na_2$ and $C_{60}Na_6$ are given in Supplementary information. They are somewhat similar to those calculated using CAM-B3LYP, but the main band obtained at B3LYP and PBE0 levels is slightly redshifted, while it is blueshifted by 0.3-0.4 eV at ω B97x, LC-M06L, LC- ω PBE levels. Pre- and postprocessing operations were performed with the graphical interface GABEDIT [45].

The present level of calculation is a good compromise between accuracy and cost. To obtain a good description of the ionic bonding between alkali atoms and C_{60} fullerene, we should have correct values of ionization potential of alkali atoms and electron affinity of C_{60} . Present IPs are calculated at 5.59, 5.36, and 4.43 eV for Li, Na, and K atoms respectively, in good agreement with the experimental data of 5.39 [46], 5.14 [47], and 4.34 [48] eV respectively. The electroaffinity of C_{60} fullerene is calculated at 1.87 eV while the experimental value ranges from 1.62 to 2.68 eV [49, 50]. Otherwise, the vertical IP of C_{60} is calculated at 7.60 eV, it is exactly the experimental value [51]. To our knowledge, the only available experimental IP of C_{60} -alkali concerns that of $C_{60}K$ for which the value would be in the 5.0-6.4 eV range [51]; the present calculated value is 4.64 eV.

3. Results and discussions

3.1 Absorption Spectra of C_{60} and C_{60}^-

Calculated absorption spectra of both neutral C_{60} and anionic C_{60}^- fullerenes are given in Figure 1. The absorption spectra of neutral C_{60} is calculated up to 7 eV, but we also show the

spectrum in the 0-5 eV range to facilitate the comparison with spectra of metal-C₆₀ presented below in the 0-5 eV range. Due to the high symmetry of C₆₀ and the closed-shell electronic structure, only few transitions are allowed. All dipole-allowed transitions are triply degenerate. They are calculated respectively at 4.28, 4.66, 5.63, 6.31 and 6.70 eV, the more intense peaks being found at 5.63 eV. Present results are in line with previous theoretical ones [52]. Comparison of the present calculated spectrum on isolated C₆₀ with experimental data is difficult since the experimental measurements have been performed either in hot gas phase [53] or embedded in a condensed medium [52, 53-56]. For examples, the experimental spectrum of C₆₀ in *n*-hexane solution at room temperature shows three wide strong bands with maximum at 3.78, 4.84 and 5.88 eV, and less intense peaks at 4.35, 5.46, 6.36 eV [54,55], while the spectrum of C₆₀ molecule in cryogenic parahydrogen solids gives main bands at 3.71, 4.82 and 5.88 eV [56]. A good discussion about the comparison experiment-theory can be found in Ref [52]. It is not the goal of the present study to describe the experimental spectrum of C₆₀. We will focus on the effects of adsorption of alkali metals on the spectrum.

In previous works [24, 25], the C₆₀M clusters were described as C₆₀⁻ + M⁺ since the valence electron of the alkali atom was completely transferred to the fullerene. Then, it could be interesting to compare the spectra of C₆₀M clusters to that of the anion C₆₀⁻. That is why we have also calculated the spectrum of the negatively charged C₆₀⁻. In Figure 1, we give the absorption spectrum of the anion at the *I_h*-symmetry structure of the neutral fullerene. In the present work, the relaxed structure of C₆₀⁻ is of *D_{3d}* symmetry, but it presents a very similar absorption spectrum to that of the *I_h*-symmetry structure. The spectrum of the anion is somewhat similar to that of neutral C₆₀, but it contains more transitions than that of the neutral specie since the extra electron modifies the electronic structure. Indeed, the degeneracies found in neutral C₆₀ of both the 5-fold degenerated HOMO (highest occupied molecular orbital) and the 3-fold degenerated LUMO (lowest unoccupied MO) are lifted up in the anion [57], leading to a broadening of the absorption band in the 4-5 eV range. Also, while the neutral C₆₀ has no dipole-allowed excitation in the infrared and visible range of the spectrum, the spectrum of C₆₀⁻ presents some weak peaks at low energy: a doubly degenerated transition at 1.14 eV associated to the singly occupied molecular orbital SOMO → LUMO + 1 excitation, and some insignificant peaks near 2.4 and 2.8 eV.

3.2 Absorption Spectra of C₆₀Li, C₆₀Na and C₆₀K

In Figure 2, we show the absorption spectra of $C_{60}Li$, $C_{60}Na$, and $C_{60}K$ clusters for the two lowest-energy configurations. We label h the adsorption site located above the center of a hexagonal site, and p the site above a pentagon. For $C_{60}Na$ and $C_{60}K$, the h geometry is the most stable while h and p configurations are degenerate for $C_{60}Li$ (Table 1). The absorption spectra are very similar for h and p configurations (Figure 2). Besides, the absorption spectra do not depend on the nature of the alkali atom. For three alkali, the absorption spectrum is very similar to that of the anion C_{60}^- with an absorption band in the 4-5 eV range and a weak peak near 1.4 eV. For h configuration, the main band presents two maxima centered at 4.15 and 4.60 eV respectively. The weak peak in the visible range is due to two excited states for which the exact position slightly changed with the alkali: 1.41 and 1.46 eV for $C_{60}Na$, 1.36 and 1.40 eV for $C_{60}K$, 1.45 and 1.51 eV for $C_{60}Li$. In all cases, the peaks are blueshifted by about 0.3 eV with respect to the doubly degenerated peak of C_{60}^- at 1.14 eV, and the presence of an alkali atom lifts the degeneracy.

To characterize the electronic excitations, we show in Figure 3 a plot of the electron density difference between the excited and the ground states for some representative main peaks. Red colored regions correspond to depletion of the electron density during the transition, while blue regions correspond to an increase of the electron density. In Figure 3, we only considered $C_{60}K$, with the h geometry, but analyses are similar for $C_{60}Na$ and $C_{60}Li$. The peaks at low energy, 1.36 and 1.40 eV for $C_{60}K$, are due to excitations of the extra electron transferred from the alkali atom to the fullerene. They correspond to $SOMO \rightarrow LUMO + 4$ and $SOMO \rightarrow LUMO + 5$ transitions, and imply carbon atoms without any participation of the alkali atom. The main band in the 4-5 eV range is due to excitations from carbon orbitals to either unoccupied orbitals of C_{60} or to alkali atoms (in Figure 3 the plots for peaks at 4.14 and 4.46 eV illustrate both cases).

3.3 Absorption Spectra of $C_{60}Li_2$ and $C_{60}Na_2$

We consider now the absorption of two lithium or sodium atoms on C_{60} , the adsorption of two K is not investigated since it was not considered in the previous study on structural properties [25]. We present only spectra for three of the lowest-energy isomers labeled respectively hhc , hhd , hhe for $C_{60}Na_2$, and hpc , ppa , ppc for $C_{60}Li_2$ (see Figure 4). These labels

are taken from our previous work [24] in which we had considered all of the possible configurations in which the two alkali atoms are on *h* or *p* sites. The five configurations in which the two alkali atoms are both on *h* sites are labeled *hh* followed by a letter *a, b, c, d, e*, going from *a* for the adjacent sites to *e* for the opposite sites. Similarly, the three configurations in which the two alkali atoms are on *p* sites are labeled *pp*, while the configurations in which one *h* and one *p* sites are occupied are labeled *hp*. For $C_{60}Na_2$, the configurations *hhc*, *hhd*, *hhe*, which only differ by the relative position of two Na atoms, were found to be degenerate (Table 1). For $C_{60}Li_2$, *hpc* was found to lie 0.03 eV below *ppa* and *ppc* configurations.

For $C_{60}Na_2$, the absorption spectra are composed of a main band in the energy range of 4-4.5 eV, redshifted by about 0.2 eV with respect to the band of $C_{60}Na$, and two less intense peaks near 1.5 eV (Figure 4). The energy gap between the latter two peaks is much larger than in the $C_{60}Na$ case, since it increases from 0.2 to 0.3 eV for *hhc* and *hhe* geometries respectively, to be compared with the value of 0.05 eV for $C_{60}Na$. One can also see the emergence of some weak transitions in the 3 – 4 eV range. The spectra for the three isomers are almost identical and do not allow to distinguish between isomers. For $C_{60}Li_2$, the situation is slightly different. The spectra have a main band centered at 4.0 eV and two weak peaks below 2 eV for which both the exact positions and the energy gap depend on the configuration. The energy gap between two peaks increases when the relative distance between Li atoms increases. The excited states are quasi degenerate in *ppa* configuration (1.97 and 2.0 eV), and well separated in *hpc* (1.61 and 1.88 eV) and *ppc* (1.22 and 1.79 eV) geometries. Therefore the *ppa* configuration can be distinguished from other.

3.4 Absorption Spectra of $C_{60}Li_6$, $C_{60}Na_6$ and $C_{60}K_6$

Previous DFT calculations have shown that the adsorption of six alkali atoms on the C_{60} molecule favor a relatively large distance with no strong metallic bonding nor a formation of a metallic droplet [17, 24,25]. Here we have selected four structures in which the metal atoms are all placed above a ring (see Figure 5). In the first one, labeled *2h3*, three alkali atoms are located above three hexagonal rings located in contact with a same hexagonal site, while the three others metal atoms are located at the opposite positions of C_{60} . In the *h6* configuration, the alkali atoms are placed above hexagonal rings on close but not adjacent sites. In the *2p3* configuration, the first three alkali atoms are placed above three pentagonal rings located in contact with a

same hexagon, the three others alkali atoms are placed at the opposite positions of C_{60} . In the last structure, labeled $p6$, the metal atoms are located above a pentagonal ring of which the positions are as close to one another as possible. The most stable structure was found to be $2h3$ for $C_{60}Na_6$ and $C_{60}K_6$, while it was $p6$ for $C_{60}Li_6$ (Table 1). They result from a balance between the electrostatic repulsion between the positively charged alkali atoms, due to the electronic charge transfer from the metal atoms to the C_{60} cage, versus the metallic bonding. Na and K atoms tend to stay as far as possible from each other in order to minimize Coulomb repulsion between the positively charged alkali atoms, while the lithium atoms tend to stay together.

The calculated absorption spectra are given in Figure 5. They are somewhat similar whatever the arrangement of the alkali atoms over the fullerene. So the absorption spectra do not allow to distinguish between different configurations. But the spectra strongly depend on the nature of the alkali. In particular, the spectra of lithium-doped C_{60} , with a main band in the energy range of 3.5–4.0 eV, differ from those of sodium-doped C_{60} , which present a band in the 0.5-1.5 eV range, and those of potassium-doped C_{60} , with a response in the 0.2–1.7 eV range. In more details, the main peaks for $C_{60}Li_6$ $p6$ are calculated at 1.76, 3.64 and 3.97 eV, the main peaks for $C_{60}Na_6$ $2h3$ is located at 1.30 and 1.37 eV, those of $C_{60}K_6$ $2h3$ is located at 0.21, 0.35 and 1.61 eV. The electronic structures of $C_{60}Na_6$ and $C_{60}K_6$ differ from that of $C_{60}Li_6$. The HOMO-LUMO gap are low: 0.06715 and 0.03694 Hartree for $C_{60}Na_6$ and $C_{60}K_6$ respectively versus 0.12214 Hartree for $C_{60}Li_6$. The ionization potential are found to be very low for $C_{60}Na_6$ and $C_{60}K_6$ (2.73 and 1.97 eV respectively) while it is calculated at 4.24 eV for $C_{60}Li_6$ (Table 1). Furthermore the nature of the LUMOs is different: the first six LUMOs (LUMO to LUMO + 5) are located on alkali atoms in cases of sodium- and potassium-doped C_{60} , while they are a mixing of atomic orbitals localized on lithium atoms and orbitals from the C_{60} molecule in the case of $C_{60}Li_6$.

In Figure 6, we show a plot of the electron density difference between the excited and the ground states for some representative main peaks for $C_{60}Na_6$ and $C_{60}Li_6$. For $C_{60}Na_6$ and $C_{60}K_6$ the peaks at low energies are due to transitions from orbitals localized on C_{60} (HOMO, HOMO-1, and HOMO-2) to orbitals on alkali atoms (LUMO, LUMO+1, LUMO+2, LUMO+3), as illustrated in Figure 6 with transitions at 0.53 and 0.84 eV. The transitions beyond 1 eV are associated to excitations on the fullerene with a weak participation of metal atoms. For $C_{60}Li_6$, all significant peaks are due to transitions from orbitals localized on carbon to orbitals on both lithium and carbon atoms. For a given excitation, we have evaluated the

spatial overlap between the occupied and virtual orbitals using the Λ diagnostic test proposed by Tozer [58]. The value of Λ , which is in the interval $[0,1]$, can be helpful to distinguish the local excitations, the Rydberg excitations and the charge-transfer excitations. A local excitation is expected to give a relatively large value while Rydberg and charge-transfer excitations are expected to be characterized by a relatively small value. In the case of $C_{60}Na_6$, our calculated values, given in Figure 6, are in the range of 0.26-0.43 for transitions associated to a charge-transfer from the C_{60} fullerene to Na atoms, and in the 0.73-0.81 range for valence excitations located on C_{60} .

3.5 Absorption Spectra of $C_{60}Li_{12}$, $C_{60}Na_{12}$ and $C_{60}K_{12}$

For higher concentration of alkali (12 alkali atoms), the behavior of sodium and potassium atoms differs from that of lithium atoms since lithium atoms homogeneously cover the surface of the C_{60} with twelve atoms on the twelve pentagonal sites, while sodium and potassium atoms prefer to form 4-atom islands [24, 25]. In the present work, we have considered the most representative isomers optimized in previous works [24, 25, 26] with a selection of initial configurations ranging from homogeneous covering of the fullerene to complete segregation with a metallic droplet, but also intermediate situations. The geometries can be seen in Figure 7. The *34-1* and *34-2* structures are made of three islands of four atoms. For each tetramer, three atoms are in contact with the C_{60} , two via a pentagonal ring and one via an adjacent hexagonal ring, while the fourth atom is capped over the other metal atoms. In the *34-1* geometry, the three small metallic islands are very close from each other, while in *34-2* they are as distant as possible. The *34-3* isomer is similar but the alkali atoms are in contact with the fullerene via two adjacent hexagonal ring and one pentagonal ring. This structure was found to be the lowest-energy isomer for sodium-decorated C_{60} by Karamanis [26]. The structure labeled *m12* consists of a metallic droplet adsorbed on the fullerene. The configuration *ic* consists in an inhomogeneous coating in which all the metal atoms are in contact with the C_{60} , five metal atoms are on the “northern” face while seven atoms are on the “southern” face. This structure is only stable for potassium-doped C_{60} . The last two geometries are labeled *p12* and *p11-1*. The twelve alkali atoms are located above the twelve pentagonal rings in the *p12* geometry. The *p11-1* configuration is obtained from *p12* after the moving of a single alkali atom from a

pentagonal site towards a hexagonal ring and capping three other alkali atoms. For the *34-1*, *34-2*, *p11-1* configurations, the optimization of Li-doped C_{60} has converged toward slightly different structures from the initial ones (see final structures in Figure 7). The lowest-energy isomer is the *34-3* structure for sodium- and potassium-doped C_{60} , while it is the *p12* structure for the lithium-doped C_{60} (Table 1).

Calculated spectra, given in Figure 7, are found to depend on both the nature of the alkali and the arrangement of the metal atoms over the fullerene. Sodium-doped C_{60} in its most stable structure (*34-3*) presents two main bands centered respectively at 2.30 and 2.55 eV and a less intense band centered at 1.40 eV. Spectra of the others isomers based on 4-atom island (*34-1* and *34-2*) are somewhat similar, while the optical response of *m12* and *p12* configurations give a strong scattering in the oscillator strengths in the ranges of 2-3.5 eV (*m12*) and 0-3.5 eV (*p12*). For the latter, the presence of many dipole-allowed transitions is explained by the symmetry breaking during the optimization, i.e. the optimization of the I_h -symmetry configuration converges into a geometry belonging to the C_{2h} symmetry but still labeled *p12*. The most stable structure of potassium-doped C_{60} (*34-3* configuration) presents two main bands centered respectively at 1.80 and 1.92 eV and a less intense band centered at 1.34 eV. The band at 1.80 eV is due to ten excited states scattered in the range of 1.70-1.86 eV, while the band at 1.92 eV is associated to two quasi degenerated excited states. The spectrum of the *m12* configuration presents a large band in 1.5-2.5 eV range. The *ic*, *p11-1* and *p12* structures, characterized by a more or less homogeneous coating, present somewhat similar spectra with some main bands centered at about 1.4 and 2.2 eV. For lithium-doped C_{60} , the *p12* configuration is much more stable than the other (Table 1). Its I_h symmetry leads to very few dipole-allowed transitions. Below the IP of 3.11 eV, only one peak is calculated at 3.04 eV (and an insignificant one at 1.43 eV). However, at higher energies we have found intense transitions at 4.07, 4.16, 4.31, 5.57, 5.64, 6.04, 6.48, and 6.93 eV. The comparison between the spectrum of the *p12* configuration and that of *p11-1* shows that the moving of a single lithium atom from a pentagonal site leads to significant changes on the spectrum since many excited states well scattered in the 0-3 eV range is visible in the spectrum of the *p11-1* structure. It is clear that the optical response of the *p12* structure differs from those of the other configurations, and can be used as a signature of its structure. Therefore, an experimental measurement of the absorption spectrum of $C_{60}Li_{12}$ would be a definitive evidence of the homogeneous coating of the fullerene

by all lithium atoms above the twelve pentagonal faces resulting in an icosahedral arrangement.

The configurations investigated here differ by the type of bonding with the quasi-fully ionic bonding in the *p12* geometry for which a population analysis has shown that $\text{Li}_{12}\text{C}_{60}$ can be described as $12\text{Li}^+ + \text{C}_{60}^{12-}$ [24], and the metallic bonding in the *m12* configuration where the metal-metal bonds stabilizes the droplet, and also intermediate situations in which metallic bonds is not strong enough to overcome the electrostatic penalty, leading to the formation of several small droplets. Surprisingly, the *m12* and *p12* configurations present somewhat similar spectra, although different, in the case of sodium- and lithium-doped C_{60} though both configurations strongly differ by the type of bonding and the electronic structure. Indeed, the shape of the spectra is somewhat similar. However, the values of the oscillator strengths differ by a factor of 10 in lithium-doped C_{60} .

The analysis of the electronic transitions in Figure 8 shows three types of excitations: transitions on C_{60} fullerene without any significant contribution from the alkali atoms (with $\Lambda \sim 0.6$), transitions localized on alkali atoms without participation of the fullerene (with $\Lambda \sim 0.6$), and transitions associated to an electron transfer from C_{60} to alkali atoms (with $\Lambda \sim 0.4$ for $\text{C}_{60}\text{Na}_{12}$ and $\text{C}_{60}\text{K}_{12}$, and $\Lambda \sim 0.25$ for $\text{C}_{60}\text{Li}_{12}$). For the most stable structure (*34-3*) of sodium-doped C_{60} , the first band at 1.40 eV is due to several excited states associated to an electron transfer from the fullerene to the metal part, as illustrated in Figure 8 with the excited state at 1.39 eV. The band centered at 2.30 eV is due to local excitations on Na_4 islands without significant contribution from carbon atoms (see the excited state at 2.29 eV in Figure 8). This is in line with previous works which measured an intense optical response close to 2.5 eV for the isolated Na_4 cluster [59,60]. Finally, the main band centered at 2.55 eV is due to a collective excitation implying all carbon and sodium atoms. For the potassium-doped C_{60} in the *34-3* configuration, the weak band at 1.34 eV is due to excitation of C_{60} (negatively charged after the transfer of several valence electrons of potassium) without any participation of potassium atoms. The band at 1.80 eV is due to several excited states associated to transitions from orbitals on both carbon and potassium atoms to unoccupied orbitals of potassium atoms. Finally, the peaks at 1.92 eV is associated to two quasi degenerated excited states, located at 1.91 and 1.93 eV respectively. They correspond to excitations localized on K_4 islands without any contribution of C_{60} . For $\text{C}_{60}\text{Li}_{12}$ in its most stable configuration (*p12*), the only strong transition

(at 3.04 eV) calculated below the IP corresponds to a transfer of electronic charges from C_{60} (negatively charged) to lithium atoms (positively charged).

4. Conclusion

We have presented the absorption spectra of the alkali-doped fullerene $C_{60}M_n$ with $M=Li, Na, K$, and $n = 1, 2, 6, 12$, in the framework of the time-dependent density-functional theory (TDDFT) using the range-separated hybrid density functional CAM-B3LYP. In few cases the absorption spectra were showed to depend on the arrangement of the alkali atoms over the fullerene, though sometimes the absorption spectra do not allow to distinguish between different configurations. When one or two alkali atoms are adsorbed on the fullerene, the optical response of alkali-doped C_{60} is similar to that of the anionic C_{60}^- with a strong response in the UV domain. When metal-metal bonds are formed, the metal- C_{60} complexes present a strong optical response in infrared and visible domains in contrast with the isolated C_{60} for which dipole-allowed excitations are only found in the UV range. This is especially evident for sodium- and potassium-doped C_{60} for which the onset of metal-metal bonding appears earlier than in lithium-doped C_{60} . For $C_{60}Li_{12}$, the I_h -symmetry structure presents a particular absorption spectrum, almost without peaks in the visible, which differs from spectra calculated for the other isomers, and then could be used as a signature of its structure since a measurement of the absorption spectrum of $C_{60}Li_{12}$ could validate the symmetry of the cluster.

Acknowledgement

The author thanks the Pôle Scientifique de Modélisation Numérique (PSMN) at Lyon, France, and the GENCI-IDRIS center for generous allocation of computational times.

References:

- [1] H. W. Kroto, J. R. Heath, S. C. O'Brien, R. F. Curl, R. E. Smalley, *Nature (London)*, 1985 **318**, 162.
- [2] A. F. Hebard, M. J. Rosseinski, R. C. Radon, D. W. Murphy, S. H. Glarum, T. T. Palstra, A. P. Ramirez, A. R. Kortan, *Nature (London)*, 1991, **350**, 600.
- [3] M. J. Rasseinsky, A. P. Ramirez, S. H. Glarum, D. W. Murphy, R. C. Haddon, A. F. Hebard, T. T. TM Palstra, A. R. Kortan, S. M. Zahurak, A. V. Makhija, *Phys. Rev. Lett.*, 1991, **66**, 2830.
- [4] M. Hirscher, M. Becher, M. Haluska, A. Quintel, V. Skakalova, Y.-M. Choi, U. Dettlaff-Weglikowska, S. Roth, I. Stepanek, P. Bernier, A. Leonhardt, J. Fink, *J. Alloy. Compd*, 2002, **330-332**, 654-658.
- [5] Q. Sun, P. Jena, Q. Wang, M. Marquez, *J. Am. Chem. Soc.*, 2006, **128**, 9741.
- [6] K. R. S. Chandrakumar, S. K. Ghosh, *NanoLetters*, 2008, **8**, 13.
- [7] Q. Peng, G. Chen, H. Mizuseki, Y. Kawazoe, *J. Chem. Phys.*, 2009 **131**, 214505.
- [8] M. M. Wu, Q. Wang, Q. Sun, P. Jena, Y. Kawazoe, *J. Chem. Phys.*, 2010, **133**, 154706.
- [9] J. A. Teprovich Jr., M. S. Wellons, R. Lascola, S.-J. Hwang, P. A. Ward, R. N. Compton, R. Zidan, *Nanoletters*, 2012, **12**, 582-589.
- [10] A. Paolone, F. Vico, F. Teocoli, S. Sanna, O. Palumbo, R. Cantelli, D. A. Knight, J. A. Teprovich Jr, R. Zidan, *J. Phys. Chem. C*, 2012, **116**, 16365-16370.
- [11] P. A. Ward, J. A. Teprovich Jr, B. Peters, J. Wheeler, R. N. Compton, R. Zidan, *J. Phys. Chem. C*, 2013, **117**, 22569-22575.
- [12] T. P. Martin, N. Malinowski, U. Zimmermann, U. Naher, H. Schaber, *J. Chem. Phys.*, 1993 **99**, 4210.
- [13] J. Kohanoff, W. Andreoni, M. Parrinello, *Chem. Phys. Lett.*, 1992, **198**, 472.
- [14] L.-S. Wang, O. Cheshnovsky, R. E. Smalley, *J. Chem. Phys.*, 1992, **96**, 4028.
- [15] P. Weis, R. D. Rainer, G. Brauchle, M. Kappes, *J. Chem. Phys.*, 1994, **100**, 5684.
- [16] Palpant, B.; Otake, A.; Hayakawa, F.; Negishi, Y.; Lee, G. H.; Nakajima, A.; Kaya, K. *Phys. Rev. B* 1999, **60**, 4509.
- [17] N. Hamamoto, J. Jitsukawa, C. Satoko, *Eur. Phys. J. D*, 2002, **19**, 211.
- [18] M. Pellarin, E. Cottancin, J. Lermé, J. L. Vialle, M. Broyer, F. Tournus, B. Masenelli, P. Melinon, *Eur. Phys. J. D*, 2003, **25**, 31.
- [19] J. Roques, F. Calvo, F. Spiegelman, C. Mijoule, *Phys. Rev. Lett.*, 2003, **90**, 075505.
- [20] J. Roques, F. Calvo, F. Spiegelman, C. Mijoule, *Phys. Rev. B*, 2003, **68**, 205412.

- [21] F. Rabilloud, R. Antoine, M. Broyer, I. Compagnon, P. Dugourd, D. Rayane, F. Calvo, F. Spiegelman, *J. Phys. Chem. C*, 2007, **111**, 17795.
- [22] E. Zurek, J. Autschbach, N. Malinowski, A. Enders, K. Kern, *ACS NANO*, 2008, **2**, 1000.
- [23] Pitarch-Ruiz, J.; Evangelisti, S.; Maynau, D. *J. Chem. Theory Comput.*, 2005, **1**, 1079.
- [24] F. Rabilloud, *J. Phys. Chem. A*, 2010, **114**, 7241.
- [25] F. Rabilloud, *Comp. Theor. Chem.*, 2011, **964**, 213-217.
- [26] P. Karamanis, C. Pouchan, *J. Phys. Chem. C*, 2012, **116**, 11808-11819.
- [27] H. B. Wang, S. J. Li, S. L. Xiu, L. Gong, G. Chen, H. Mizuseki, Y. Kawazoe, *J. Chem. Phys.*, 2012, **136**, 174314.
- [28] M. Robledo, F. Martin, M. Alcamí, S. Diaz-Tendero, *Theor. Chem. Acc*, 2013, **132**, 1346.
- [29] A. D. Becke, *J. Chem. Phys.*, 1993, **98**, 5648.
- [30] C. Lee, W. Yang, R. G. Parr, *Phys. Rev. B*, 1988, **37**, 785.
- [31] M. J. Frisch et al. Gaussian09, Revision B.01, Gaussian, Inc., Wallingford, CT, 2010.
- [32] E. Runge and E. K. U. Gross, *Phys. Rev. Lett.*, 1984, **52**, 997.
- [33] R. van Leeuwen, *Int. J. Mod. Phys. B*, 2001, **15**, 1969.
- [34] M. E. Casida, in *Recent Advances in Density Functional Methods. Part I*, p. 155 (D.P. Chong Ed. (Singapore, World Scientific), 1995).
- [35] F. Rabilloud, *J. Phys. Chem. A*, 2013, **117**, 4267-4278.
- [36] T. Yanai, D. P. Tew, N. C. Handy, *Chem. Phys. Lett.*, 2004, **393**, 51-57.
- [37] J.D. Dill and J.A. Pople, *J. Chem. Phys.*, 1975, **62**, 2921.
- [38] M.M. Francl, W.J. Pietro, W.J. Hehre, J.S. Binkley, M.S. Gordon, D.J. DeFrees and J.A. Pople, *J. Chem. Phys.*, 1982, **77**, 3654.
- [39] V. Rassolov, J.A. Pople, M. Ratner and T.L. Windus, *J. Chem. Phys.*, 1998, **109**, 1223.
- [40] C. Adamo, V. Barone, *J. Chem. Phys.*, 1999, **110**, 6158-69.
- [41] J. D. Chai, M. Head-Gordon, *J. Chem. Phys.*, 2008, **128**, 084106.
- [42] H. Iikura, T. Tsuneda, T. Yanai, K. Hirao, *J. Chem. Phys.*, 2001, **115**, 3540-3544.
- [43] Y. Zhao, D. G. Truhlar, *J. Chem. Phys.*, 2006, **125**, 194101.
- [44] O. A. Vydrov, J. Heyd, A. V. Kruckau, G. E. Scuseria, *J. Chem. Phys.*, 2006, **125**, 074106.
- [45] A. R. Allouche, *J. Comp. Chem.*, 2011, **32**, 174-182.
- [46] B. A. Bushaw, W. Notershauser, G.W.F. Drake, H.-J. Kluge, *Phys. Rev. A*, 2007, **75**, 052503.
- [47] J. F. Baugh, C. E. Burkhardt, J. J. Leventhal, *Phys. Rev. A*, 1998, **58**, 1585-1588.

- [48] J. Sugar, C. Corliss, *J. Phys. Ref. Data*, 1985, **14**, 1-664.
- [49] G. Chen, S. Ma, R. G. Cooks, H. E. Bronstein, M. D. Best, L. T. Scott, *J. Mass. Spectrom.* 1997, **32**, 1305.
- [50] X.-B. Wang, H.-K. Woo, L.-S. Wang, *J. Chem. Phys.*, 2005, **123**, 051106.
- [51] P. Weiss, R. D. Beck, G. Brauchle, M. M. Kappes, *J. Chem. Phys.*, 1994, **100**, 5684-5695.
- [52] E. Menendez-Proupin, A. Delgado, A. L. Montero-Alejo, J. M. Garcia de la Vega, *Chem. Phys. Lett.*, 2014, **593**, 72-76.
- [53] A. L. Smith *J. Phys. B: At. Mol. Opt. Phys.*, 1996, **29**, 4975-4980.
- [54] R. Bauernschmitt, R. Ahlrichs, F. H. Hennich, M. M. Kappes, *J. Am. Chem. Soc.*, 1998, **120**, 5052-5059.
- [55] V. S. Pavlovich, E. M. Shpilevsky, *J. Appl. Spectros.*, 2010, **77**, 335-342.
- [56] N. Sogoshi, Y. Kato, T. Wakabayashi, T. Momose, S. Tam, M. E. Derose, M. E. Fajardo, *J. Phys. Chem. A*, 2000, **104**, 3733-3742.
- [57] W. H. Green Jr, S. M. Gorun, G. Fitzgerald, P. W. Fowler, A. Ceulemans, B. Titeca, *J. Phys. Chem. A*, 1996, **100**, 14892.
- [58] D. J. Tozer, N. C. Handy, *J. Chem. Phys.*, 1998, **108**, 2545.
- [59] J.-O. Joswig, L. O. Tunturivuori, R. M. Nieminen, *J. Chem. Phys.*, 2008, **128**, 014707.
- [60] G. Pal, G. Lefkidis, H. C. Schneider, W. Hubner, *J. Chem Phys.*, 2010, **133**, 154309.

Table 1. Relative energies (in eV) of lowest-energy isomers at B3LYP level (taken from Ref [24, 25]) and calculated vertical ionization potential (IP) at CAM-B3LYP/6-31G(d) level.

Species	Isomer	Relative Energy	IP
C ₆₀ Na	<i>h</i>	0.00	4.87
	<i>p</i>	0.045	
C ₆₀ Na ₂	<i>hhc</i>	0.00	4.38
	<i>hhd</i>	0.00	
	<i>hhe</i>	0.00	
C ₆₀ Na ₆	<i>2h3</i>	0.00	2.73
	<i>h6</i>	0.08	
	<i>2p3</i>	0.50	
	<i>p6</i>	0.50	
C ₆₀ Na ₁₂	<i>34-3</i>	0.00	3.37
	<i>34-2</i>	0.82	
	<i>34-1</i>	0.68	
	<i>m12</i>	1.41	
	<i>p12</i>	3.09	
C ₆₀ Li	<i>h</i>	0.0	5.12
	<i>p</i>	0.0	
C ₆₀ Li ₂	<i>hpc</i>	0.0	4.85
	<i>ppa</i>	0.03	
	<i>ppc</i>	0.03	
C ₆₀ Li ₆	<i>2h3</i>	0.98	
	<i>h6</i>	0.96	
	<i>2p3</i>	0.73	
	<i>p6</i>	0.00	4.24
C ₆₀ Li ₁₂	<i>p12</i>	0.00	3.11
	<i>34-2</i>	1.96	
	<i>34-1</i>	1.77	
	<i>ic</i>	2.93	
	<i>m12</i>	2.54	
C ₆₀ K	<i>p11-1</i>	1.03	
	<i>h</i>	0.00	4.64
	<i>p</i>	0.04	
C ₆₀ K ₆	<i>2h3</i>	0.00	1.97
	<i>h6</i>	0.16	
	<i>2p3</i>	0.29	
	<i>p6</i>	0.48	
C ₆₀ K ₁₂	<i>34-3</i>	0.00	2.48
	<i>34-2</i>	0.51	
	<i>34-1</i>	0.48	
	<i>m12</i>	1.54	
	<i>ic</i>	0.57	
	<i>p11-1</i>	1.32	
	<i>p12</i>	1.58	

Figures Captions:

Figure 1. Absorption spectra of C_{60} and C_{60}^- fullerenes.

Figure 2. Absorption spectra of $C_{60}Na$, $C_{60}K$ and $C_{60}Li$.

Figure 3. Isosurface of the electron density difference between the excited and ground states for some representative peaks of $C_{60}K$. For each transition, three isovalues are considered (0.0005, 0.0003, and 0.0001 a.u. respectively). Red regions correspond to the depletion of the electron density during the transition while the blue regions correspond to the accumulation of electrons.

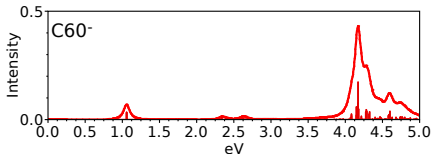
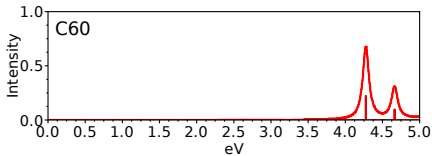
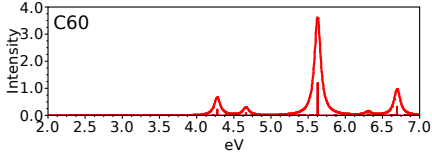
Figure 4. Absorption spectra of $C_{60}Na_2$ and $C_{60}Li_2$.

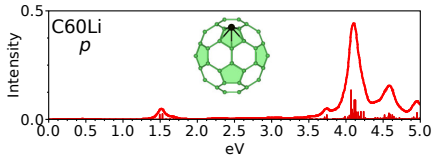
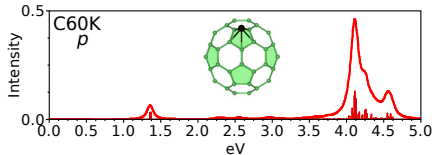
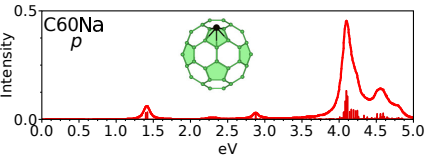
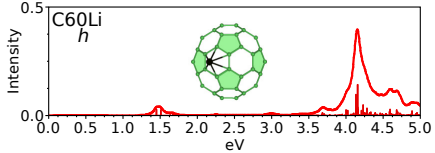
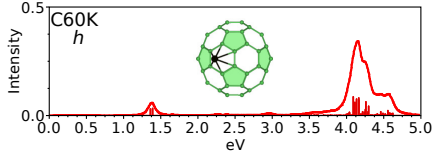
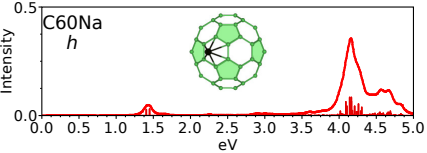
Figure 5. Absorption spectra of $C_{60}Na_6$, $C_{60}K_6$ and $C_{60}Li_6$.

Figure 6. Isosurface of the electron density difference between the excited and ground states for some representative peaks of the most stable structure of $C_{60}Na_6$ and $C_{60}Li_6$. For each transition, three isovalues are considered (0.0005, 0.0003, and 0.0001 a.u. respectively). Red regions correspond to the depletion of the electron density during the transition while the blue regions correspond to the accumulation of electrons.

Figure 7. Absorption spectra of $C_{60}Na_{12}$, $C_{60}K_{12}$ and $C_{60}Li_{12}$.

Figure 8. Isosurface of the electron density difference between the excited and ground states for some representative peaks of the most stable structure of $C_{60}Na_{12}$, $C_{60}K_{12}$, and $C_{60}Li_{12}$. For each transition, three isovalues are considered (0.0005, 0.0003, and 0.0001 a.u. respectively). Red regions correspond to the depletion of the electron density during the transition while the blue regions correspond to the accumulation of electrons.

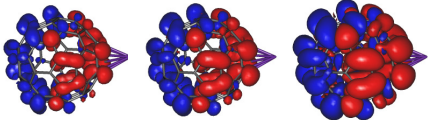




$C_{60} K h$

1.40 eV

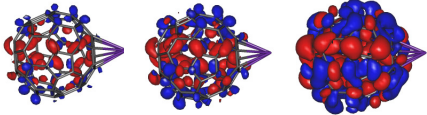
$\Lambda=0.74$



$C_{60} K h$

4.14 eV

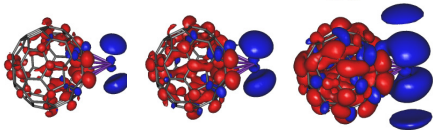
$\Lambda=0.65$

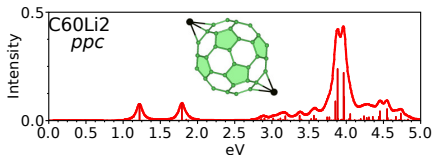
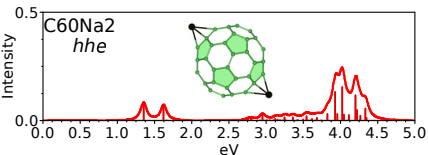
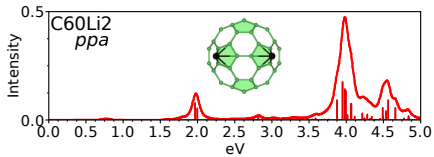
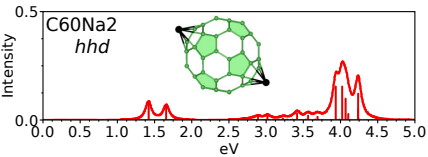
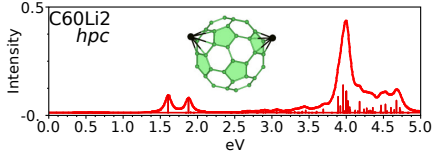
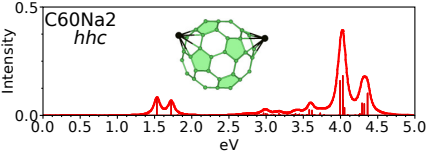


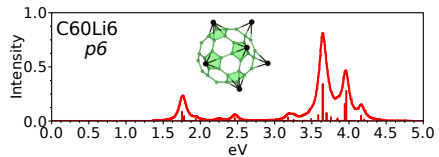
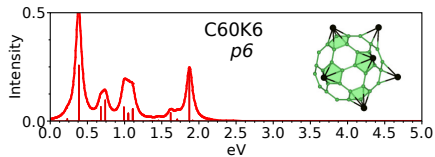
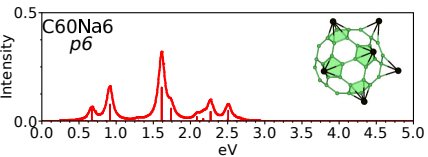
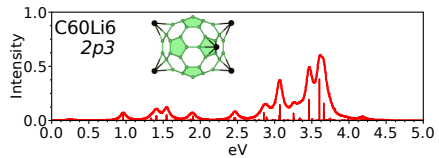
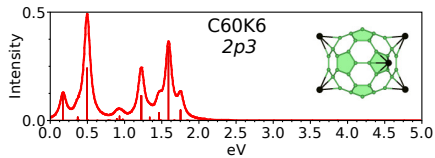
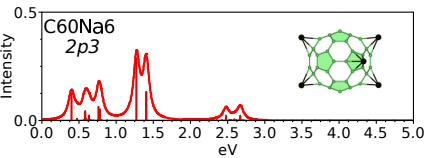
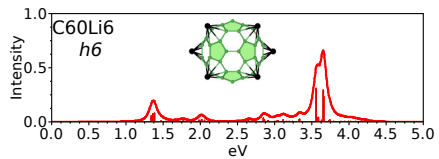
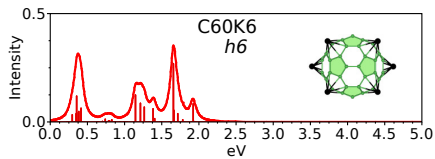
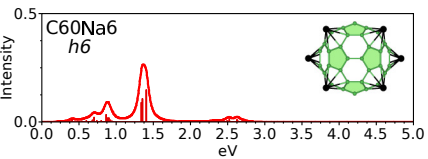
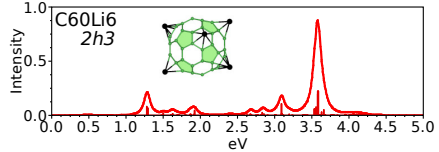
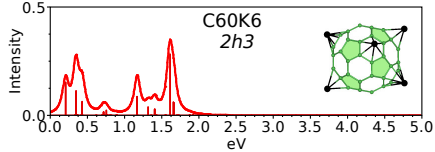
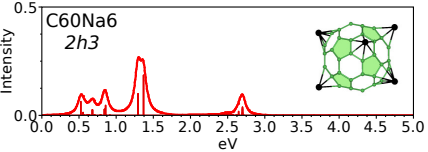
$C_{60} K h$

4.46 eV

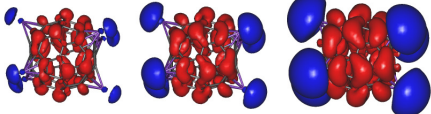
$\Lambda=0.69$



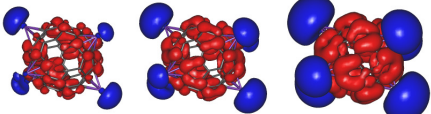




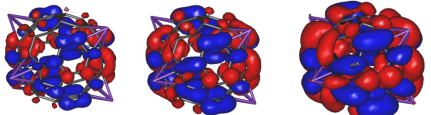
$C_{60}Na_6$ $2h3$
0.53 eV
 $\Lambda=0.43$



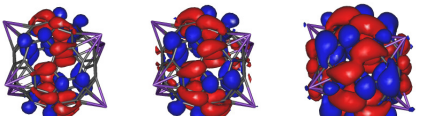
$C_{60}Na_6$ $2h3$
0.84 eV
 $\Lambda=0.26$



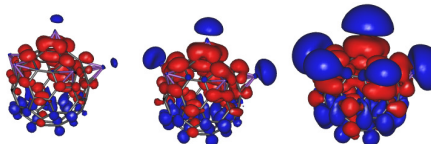
$C_{60}Na_6$ $2h3$
1.30 eV
 $\Lambda=0.81$



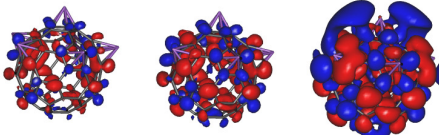
$C_{60}Na_6$ $2h3$
1.37 eV
 $\Lambda=0.73$



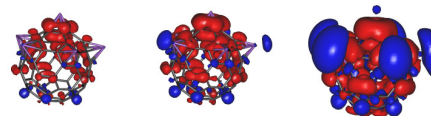
$C_{60}Li_6$ $p6$
1.76 eV
 $\Lambda=0.56$

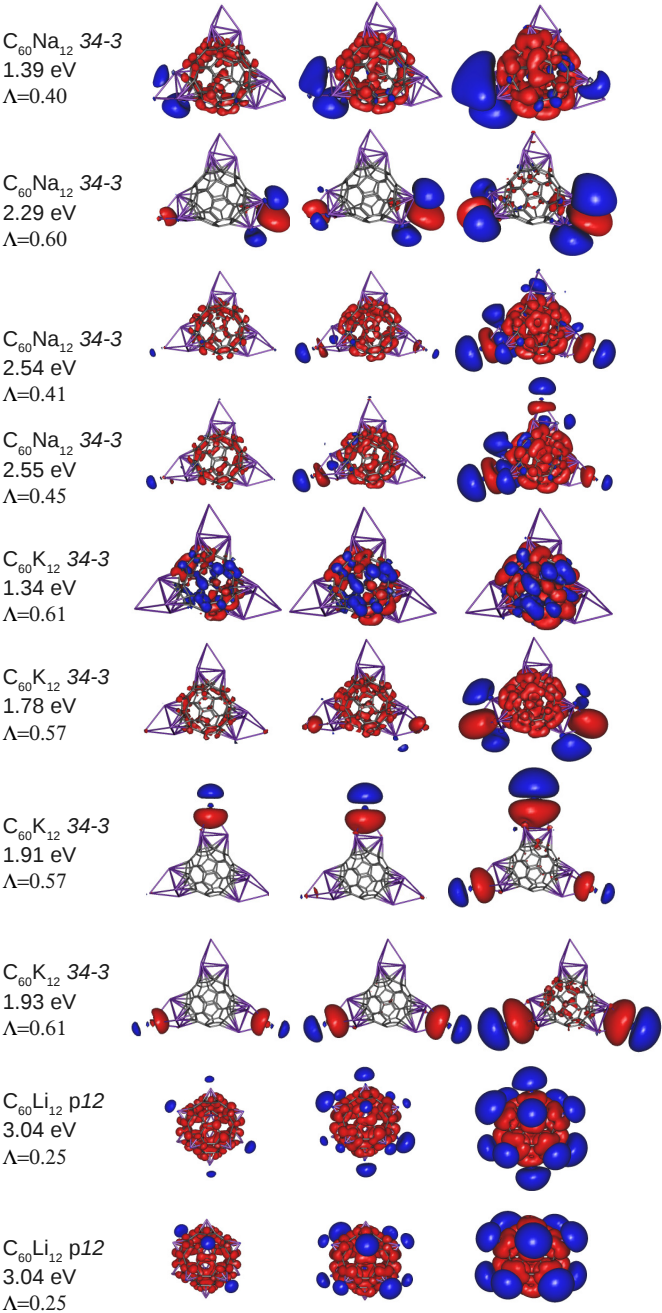


$C_{60}Li_6$ $p6$
3.64 eV
 $\Lambda=0.56$



$C_{60}Li_6$ $p6$
3.97 eV
 $\Lambda=0.59$





Absorption spectra of alkali-C₆₀ nanoclusters

Franck Rabilloud

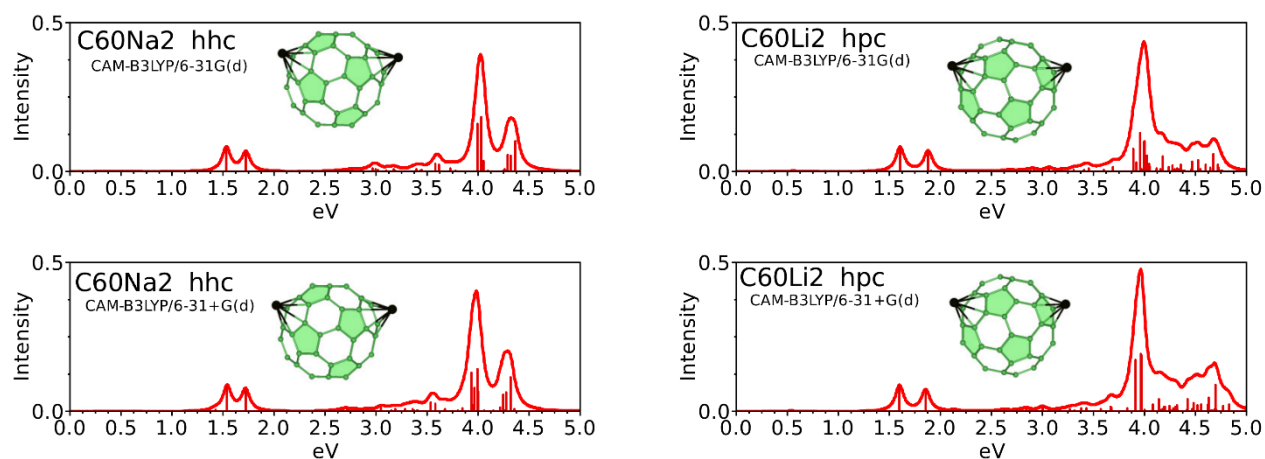
Institut Lumière Matière, UMR5306 Université Lyon 1 – CNRS,

Université de Lyon, 69622 Villeurbanne Cedex, France;

franck.rabilloud@univ-lyon1.fr

Supplementary information

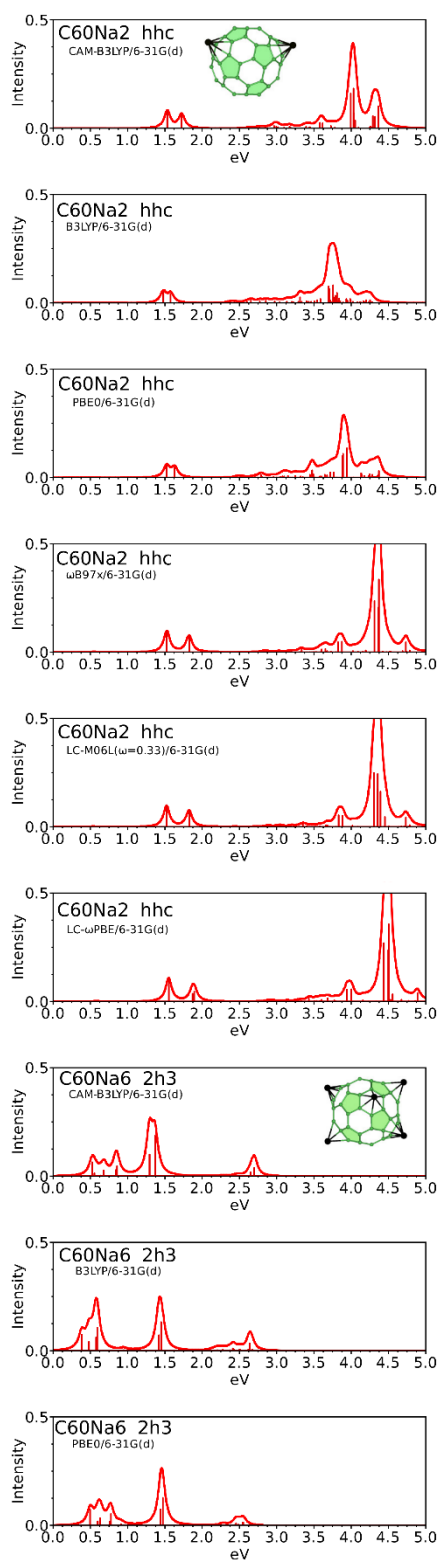
Figure S-1.



Absorption spectra of C₆₀Li₂ and C₆₀Na₂ calculated with CAM-B3LYP and using two Gaussian basis sets, namely 6-31G(d) and 6-31+G(d) [1]. Spectra are found to be very similar.

[1] J.D. Dill and J.A. Pople, *J. Chem. Phys.*, 1975, **62**, 2921; M.M. Francl, W.J. Pietro, W.J. Hehre, J.S. Binkley, M.S. Gordon, D.J. DeFrees and J.A. Pople, *J. Chem. Phys.*, 1982, **77**, 3654; V. Rassolov, J.A. Pople, M. Ratner and T.L. Windus, *J. Chem. Phys.*, 1998, **109**, 1223.

Figure S-2.



Spectra of C₆₀Na₂ and C₆₀Na₆ calculated with several exchange and correlation functionals:

the hybrid B3LYP [2] and PBE0 [3], and the long-range-corrected ones ω B97x [4], LC-M06L($\omega=0.33$) [5], LC- ω PBE($\omega=0.40$) [6], and CAM-B3LYP [7].

Spectra are somewhat similar. In comparison with spectra calculated at CAM-B3LYP level, the main band obtained at B3LYP and PBE0 levels is slightly redshifted, while it is blueshifted by 0.3-0.4 eV at ω B97x, LC-M06L, LC- ω PBE levels.

[2] A. D. Becke, *J. Chem. Phys.*, 1993, **98**, 5648; C. Lee, W. Yang, R. G. Parr, *Phys. Rev. B*, 1988, **37**, 785.

[3] C. Adamo, V. Barone, *J. Chem. Phys.*, 1999, **110**, 6158-69.

[4] J. D. Chai, M. Head-Gordon, *J. Chem. Phys.*, 2008, **128**, 084106.

[5] H. Iikura, T. Tsuneda, T. Yanai, K. Hirao, *J. Chem. Phys.*, 2001, **115**, 3540-3544; Y. Zhao, D. G. Truhlar, *J. Chem. Phys.*, 2006, **125**, 194101.

[6] O. A. Vydrov, J. Heyd, A. V. Krukau, G. E. Scuseria, *J. Chem. Phys.*, 2006, **125**, 074106.

[7] T. Yanai, D. P. Tew, N. C. Handy, *Chem. Phys. Lett.*, 2004, **393**, 51-57.